small tilt makes it difficult to explain the origin of the field in terms of classical dynamo theory (5). The absence of tilt coupled with the lack of surface detail also makes it difficult to determine an exact rotational period for Saturn. The magnetic field measurements and the celestial mechanics results are consistent with a model for the interior of Saturn that has a small inner core of about 0.2 $R_S$, consisting of rocky material such as MgO, $SiO_2$, FeS, and FeO, surrounded by an outer core of metallic hydrogen extending from 0.2 to 0.5 $R_S$, and that in turn surrounded by a liquid hydrogen-helium outer envelope. The 0.5-$R_S$ core is considerably smaller than the 0.75-$R_J$ (1 $R_J$ = 71,400 km) core at Jupiter.

*Magnetosphere*. The magnetic field of Saturn has created a magnetosphere intermediate in size between the magnetospheres of Earth and Jupiter. The bow shock wave was first encountered near 24 $R_S$. The bow shock was again crossed at 23.1 and at 19.9 $R_S$ before the magnetopause was crossed at 17.3 $R_S$. Solar activity in late August increased the solar wind pressure on the magnetic field, resulting in compression of the magnetosphere to less than its quiet time standoff distance. Pioneer entered the magnetosphere near the noon meridian and exited along the dawn meridian. The effects of the solar disturbance had largely passed by the time Pioneer exited the magnetosphere. As a consequence, magnetospheric boundaries were moving much more rapidly than they do during periods of high solar wind pressure. On the outbound leg, the magnetopause was crossed five times between 30.25 and 39.81 $R_S$ and the bow shock was crossed nine times between 49.26 and 102 $R_S$.

The magnetosphere itself can be divided into four parts: the outer magnetosphere, the slot, the inner magnetosphere, and the rings. The outer magnetosphere contained, at the time of the encounter, an inflated corotating plasma. The ions $O^+$ or $OH^+$ have been tentatively identified. This is a strong indication that the low-energy particles originated from dissociated ring material rather than from the penetration of solar wind ions into the magnetosphere. Low-energy trapped charged particles were found inside 17 $R_S$ and extended inward to about 7.5 $R_S$. The outer magnetosphere is characterized by large, time-varying fluxes of trapped particles, with large variations in their angular distribution. During the outbound leg beyond 8 $R_S$ a chaotic particle distribution and a rapidly changing magnetic field polarity was encountered. This has been attributed to the development of an equatorial current sheet or the detection of a magnetospheric tail current sheet. The outer magnetosphere is terminated sharply at 7.5 $R_S$ by a sudden drop in both the proton and electron fluxes. The slot region resulting from the reduction in particle flux is attributable to strong particle absorption by the satellites Dione, Tethys, and Enceladus. The slot extends in to 4 $R_S$. The charged particle data contain evidence that plasma processes, as well as satellite absorption, are sweeping charged particles out of the magnetosphere in the slot region.

Inside 4 $R_S$, particle fluxes and energies increase and the spectra become much harder and more complex. Maximum flux for protons with energies greater than 35 MeV is $3 \times 10^4$ $cm^{-2}$ $sec^{-1}$ and for electrons with energies greater than 3.4 MeV is $3 \times 10^6$ $cm^{-2}$ $sec^{-1}$. The charged particles trapped in the inner magnetosphere show strong symmetry between the inbound and outbound legs of the encounter. This is a direct consequence of the coincidence of the magnetic axis with the rotational axis of the planet. A distinct absorption feature in the particle fluxes was found associated with the satellite Mimas at 3.1 $R_S$. Particle absorption features were also used to discover one and possibly more previously known Saturn satellites and to place an upper limit on the diffusion coefficient for trapped particles in that region of the magnetosphere. The magnetospheric environment of the rings is characterized by the virtually complete absence of any charged particle radiation. Inside 2.3 $R_S$, the outer edge of the A ring, there is a nearly complete dropout of particles. Searches for the photon radiation resulting from the high-energy particle absorption have yielded negative results.

*Summary*. The spacecraft and instruments all survived passage through the rings of Saturn. Pioneer established that subsequent missions to the outer planets, such as those of Voyager 1 and Voyager 2, will be able to survive an outside crossing of the Saturn rings as well as the trapped radiation environments. Pioneer Saturn continues to provide scientific data on the interplanetary medium. The spacecraft is presently traveling in the direction of the apex of the solar wind interaction with the interstellar medium. Spacecraft power and tracking capability are adequate to continue data acquisition into the middle 1980's.

ALBERT G. OPP
*National Aeronautics and Space Administration, Washington, D.C. 20546*

**References**

1. T. Gehrels *et al.*, *Science* **207**, 434 (1980).
2. J. W. Fountain and S. M. Larson, *Icarus* **36**, 92 (1978).
3. L. W. Brown, *Astrophys. J.* **198**, L89 (1975).
4. M. L. Kaiser and R. G. Stone, *Science* **189**, 285 (1975).
5. T. G. Cowling, *Magnetohydrodynamics* (Interscience, New York, 1957), p. 78.

3 December 1979

## Preliminary Results on the Plasma Environment of Saturn from the Pioneer 11 Plasma Analyzer Experiment

Abstract. *The Ames Research Center Pioneer 11 plasma analyzer experiment provided measurements of the solar wind interaction with Saturn and the character of the plasma environment within Saturn's magnetosphere. It is shown that Saturn has a detached bow shock wave and magnetopause quite similar to those at Earth and Jupiter. The scale size of the interaction region for Saturn is roughly one-third that at Jupiter, but Saturn's magnetosphere is equally responsive to changes in the solar wind dynamic pressure. Saturn's outer magnetosphere is inflated, as evidenced by the observation of large fluxes of corotating plasma. It is postulated that Saturn's magnetosphere may undergo a large expansion when the solar wind pressure is greatly diminished by the presence of Jupiter's extended magnetospheric tail when the two planets are approximately aligned along the same solar radial vector.*

The Pioneer 11 spacecraft, launched on 6 April 1973, passed at a distance of 1.35 $R_S$ (Saturn radii; 1 $R_S$ = 60,000 km) from the center of the planet at 1631 UT (spacecraft time) on 1 September 1979. The Ames Research Center plasma analyzer experiment on Pioneer 11, identical to that on Pioneer 10 (*1*), utilizes dual, 90°, quadrispherical electrostatic analyzers for measurements of the energy and direction of motion of the charged particles that comprise the incident plasma. The experiment includes a medium-resolution analyzer that incorporates five current collectors and attendant electrometer amplifiers for charged particle detection, and a high-resolution analyzer that has 26 Bendix-type CEM 4012 detectors operated in the pulse counting mode. The plasma analyzer ex-


0036-8075/80/0125-0403$01.00/0 

periment covers the energy range from 100 to 18,000 eV for protons and approximately 1 to 500 eV for electrons. The experiment views back toward Earth along the spacecraft spin axis, so that as the spacecraft rotates (approximately 7.8 rev/min during the Saturn encounter) the azimuthal angle of incidence of the solar wind is measured by the spacecraft roll position, while the angle with respect to the spin axis is measured by the multiple detector system of the instrument.

After the Pioneer 11 encounter with Jupiter on 3 December 1974 (*2*), an in-flight interference test was conducted on the spacecraft, during which the plasma analyzer experiment was turned off for 4 days. The instrument was reactivated on 16 April 1975 but failed to provide a valid data output. The early attempts to correct this malfunction were not successful. A study was performed in which it was determined that the malfunction was most likely located in the digital logic section of the instrument and was probably due to a combination of radiation damage at Jupiter and the low temperature reached during the period when the instrument was turned off. Finally, in late October 1977, a series of power off-on and other commands was sent to the experiment and it returned to nominal operation on 3 December 1977. Since that time, and all through the Saturn encounter, the experiment has operated normally in all respects.

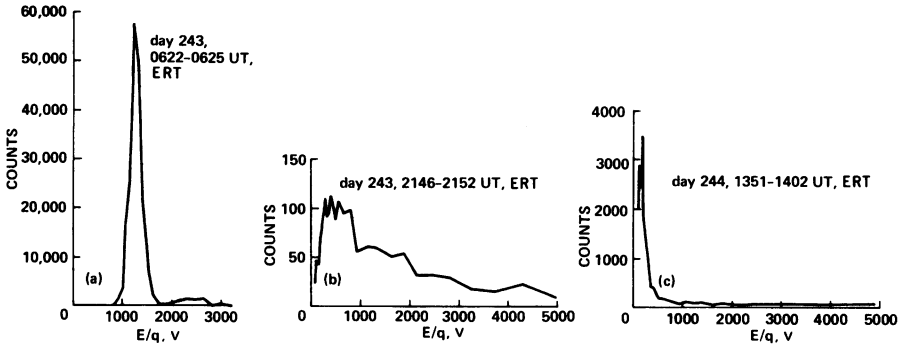


Fig. 1. Comparison of solar wind ion spectra taken (a) upstream and (b) downstream from Saturn's bow shock during the inbound part of the flyby of Pioneer 11 past Saturn. (c) Spectrum that shows the highest flux of corotating plasma observed within Saturn's magnetosphere.

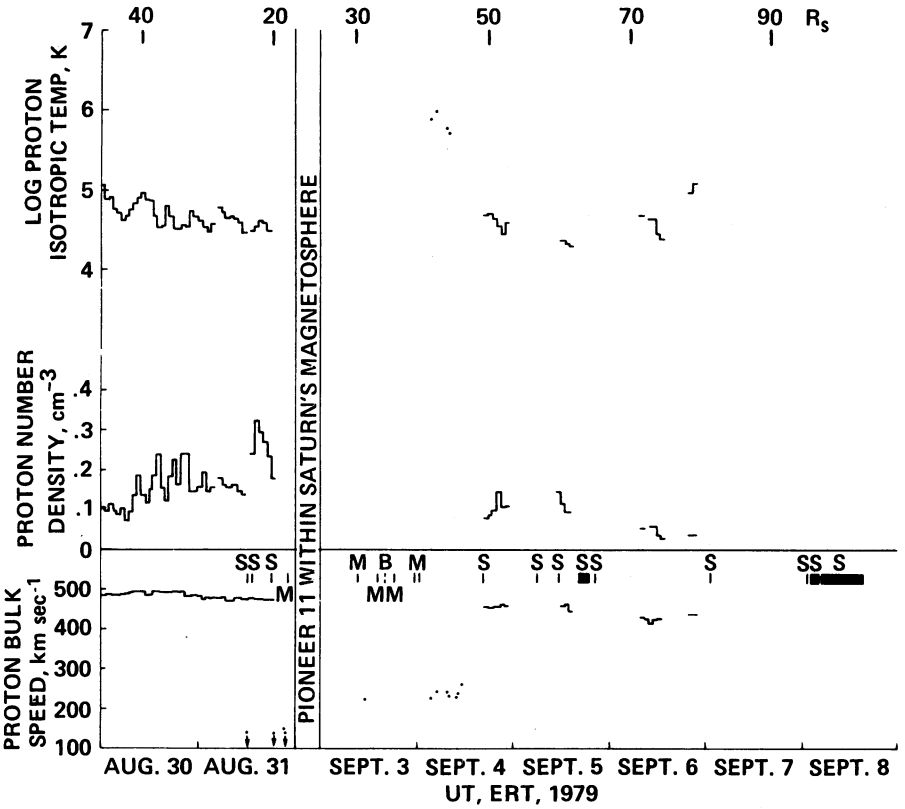


Fig. 2. Hourly averages of solar wind parameters before and after the closest approach of Pioneer 11 to Saturn, as well as examples of magnetosheath proton bulk speeds or upper limits and magnetosheath proton temperatures. Times of bow shock (*S*) and magnetopause (*M*) crossings are also indicated; (*B*) denotes a plasma burst.

*Observations*. As the Pioneer 11 spacecraft approached Saturn, the first indication of the interaction of the solar wind with the planet occurred at 1209 UT, Earth received time (ERT) on 31 August 1979. At that time the spacecraft was 24.1 $R_S$ upstream from the center of the planet, approaching in the late morning quadrant (*3*). Here, within one cycle time of the plasma analyzer experiment (approximately 3.5 minutes), the plasma ion spectrum changed from a typical interplanetary appearance (Fig. 1a) to that characteristic of a postshock or magnetosheath flow (Fig. 1b). The solar wind speed was observed to decrease from 470 to less than 140 km $sec^{-1}$, with a corresponding increase in temperature from 30,000 to nearly $5 \times 10^5$ K (although the distribution function does not appear to be Maxwellian). At the same time, the density increased by at least a factor of 3. Coincident with these changes in plasma ion parameters, the flow direction was observed to change from approximately antisolar to an angle of about 30° with respect to the sun-spacecraft line. This well-defined transition is identified as the presence of a detached, strong, bow shock wave standing off from Saturn's magnetosphere.

The example of the magnetosheath spectrum shown in Fig. 1b reveals the low velocity and high temperature profile typically observed behind Saturn's bow shock throughout the encounter. This spectrum was obtained at a distance of 17.6 $R_S$ during the inbound pass of Pioneer 11. The ragged appearance of the peak of the spectrum may be due to sample aliasing caused by fluctuations in the parameters of the plasma flow in Saturn's magnetosheath. Detailed examination of a number of these spectra suggests increased fluctuations in the low-energy range. The spectrum presented may also show a nonthermal tail or heated solar wind helium, or both.

At the magnetopause boundary between the magnetosheath flow field and Saturn's magnetosphere, the postshock convecting plasma was observed to cease; the exclusion of the magnetosheath flow from Saturn's magnetosphere appears quite similar to the cases at Earth and Jupiter. Within Saturn's magnetosphere, a new plasma regime was encountered, whose flow appears consistent with corotation with Saturn's

magnetic field. An example of an ion spectrum was obtained by the high-resolution analyzer at 4.9 $R_S$ on the inbound leg. The bifurcated appearance near the peak and the low apparent speed of this peak were repeated in many of the spectra for the corotating plasma.

During the Pioneer 11 encounter, Saturn's bow shock was crossed three times on the inbound pass and at least nine times outbound. The magnetopause was crossed only once inbound but at least five times outbound. Table 1 gives the Earth received times (UT) and distances from the center of Saturn of the various boundary crossings (shock and magnetopause) observed in the plasma analyzer data. Inbound bow shock crossings are detected by a pronounced shift of the plasma flow direction and an increase in temperature, so that the outermost channel multiplier of the high-resolution analyzer begins to have appreciable count rates. Magnetopause crossings are generally detected as a location with magnetosheath plasma on one side and no detectable plasma on the other. This description must be modified in the case of the inbound magnetopause, as corotating magnetospheric plasma is detected immediately after the magnetosheath plasma disappears. Such a situation has also been reported at Jupiter from the Voyager 2 results (*4*). In the case of the third outbound Saturn magnetopause crossing, the assignment was made on the basis of an increase of plasma flux over very low, sporadic values apparently observed during at least the preceding hour. The observation of corotating magnetospheric plasma was not expected on the outbound trajectory because the plasma analyzer aperture was not oriented in the favorable direction. There are large uncertainties in the time of observation for some of the final outbound shock crossings because of decreased spacecraft telemetry bit rates and increased noise in the ground receiving system due to the approach of superior conjunction. Such uncertainties imply that additional outbound shock crossings may have occurred that could not be identified in the plasma analyzer data.

Table 1. Saturn bow shock and magnetopause crossings as detected by the plasma analyzer experiment.

| Boundary | Date (1979) | Earth received time (UT) | $R_S$ |
|---|---|---|---|
| | | *Inbound* | |
| Shock 1 | 31 August | 1207:54-1209:30 | 24.1 |
| Shock 2 | 31 August | 1324 ± 30 seconds | 23.1 |
| Shock 3 | 31 August | 1813:55-1816* | 20.0 |
| Magnetopause | 31 August | 2208:55 | 17.3 |
| | | *Outbound* | |
| Magnetopause 1 | 3 September | 0916:19-0927:19 | 30.25 ± 0.06 |
| Magnetopause 2 | 3 September | 1406:55-1412:31 | 33.24 ± 0.03 |
| Plasma burst | 3 September | ~1627 | 34.7 |
| Magnetopause 3 | 3 September | 1828:43† | 35.9 |
| Magnetopause 4 | 3 September | 2334:07-2335.31 | 39.0 |
| Magnetopause 5 | 4 September | 0048:56-0103:31 | 39.81 ± 0.07 |
| Shock 1 | 4 September | 1653-1655 | 49.26 ± 0.01 |
| Shock 2 | 5 September | 0557-0609 | 56.8-56.9 |
| Shock 3 | 5 September | 1119-1124 | 59.9 |
| Shock 4 | 5 September | 1521-~1825 | 62.2-~63.9 |
| Shock 5 | 5 September | 1911-~1954 | 64.3-~64.8 |
| Shock 6 | 7 September | 0120 | 81.2 |
| Shock 7 | 8 September | 0154:07-0207:19 | 94.7-94.8 |
| Shock 8 | 8 September | 0213:55-0403:18 | 94.9-95.9 |
| Shock 9 | 8 September | 0416:30-1530 | 96.0-102.1 |

*Possible multiple crossings. †Very low plasma fluxes detected earlier.

Figure 2 shows hourly averages of proton bulk speeds (uncorrected for aberration), observed number densities, and isotropic temperatures, both before and after the closest approach of Pioneer 11 to Saturn. Bow shock and magnetopause crossings are indicated with *S* and *M*, respectively. The two days (1 and 2 September 1979) during which Pioneer 11 was within Saturn's magnetosphere are deleted from the time scale. The solar wind dynamic pressure on the inbound trajectory was quite high, ranging up to $1.5 \times 10^{-9}$ dyne cm$^{-2}$ before the final inbound bow shock crossing, compared to a normal pressure of less than $2 \times 10^{-10}$ dyne cm$^{-2}$ expected for this heliocentric distance. These pressures followed the onset of an interplanetary disturbance (corotating interaction region) that occurred at Pioneer 11 on 28 August 1979. The data also indicate that a temporary solar wind dynamic pressure increase that peaked just after 1200 UT, ERT, on 31 August 1979 produced a recession of Saturn's bow shock back past Pioneer 11 at 1324 UT, ERT, so that the spacecraft was within the free-stream solar wind again. These dynamic pressures appear much reduced on the outbound trajectory of Pioneer 11, reaching $1 \times 10^{-10}$ dyne cm$^{-2}$ late on 6 September 1979.

Figure 2 also shows a few estimates of proton bulk speeds (uncorrected for ab-

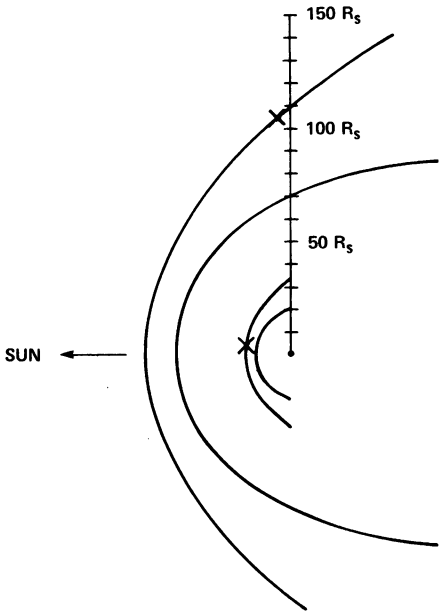


Fig. 3. Hypothetical bow shock and magnetosphere boundary surfaces for a gas dynamic analog for solar wind interaction with a planetary magnetic field. The locations of the surfaces correspond to the outermost and innermost locations, indicated by crosses, at which Saturn's bow shock was observed. Aberration is accounted for. The view is from the north, onto the plane defined by the Pioneer 11 location, Saturn, and the upstream solar wind direction.

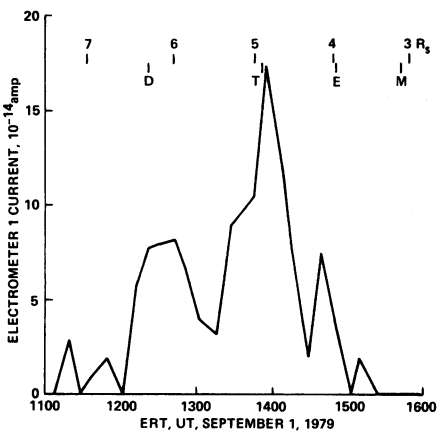


Fig. 4. Peak electrometer currents due to plasma observed from the direction of corotation within Saturn's magnetosphere. The Saturn-centered distance of Pioneer 11 and the radial distances of the moons Dione (*D*), Tethys (*T*), Enceladus (*E*), and Mimas (*M*) are also given.

erration) and temperatures in Saturn's magnetosheath. For the temperature estimates a Maxwellian velocity distribution function was assumed; however, the reader is cautioned that the observed velocity distribution functions usually appear to be non-Maxwellian. The proton bulk speeds appear to lie below the lower limit of the plasma analyzer energy range (corresponding to approximately 140 km $sec^{-1}$) for the first and most of the second, or final, inbound traversal of Saturn's magnetosheath. Estimated proton bulk speeds during some of the outbound traversals lie in the range 220 to 270 km $sec^{-1}$. These higher magnetosheath speeds are generally consistent with the spacecraft location along the flank of the magnetosphere.

Figure 3 shows minimum and maximum bow shock and magnetopause locations, with hypothetical shapes for a gas dynamic analog, based on the bow shock crossings observed nearest to and farthest from Saturn during the Pioneer 11 encounter. The locations of these bow shock crossings are indicated with crosses. The ratio of magnetosphere scale sizes for these two extremes is about 3.2 to 1, which corresponds roughly to a factor of $10^3$ difference in upstream dynamic pressure between the two cases. The distance of about 65 $R_S$ to the nose of the bow shock for the lowest-pressure case (farthest out) is close to the value predicted by Dryer *et al.* (*5*), based on a much higher dipole moment for Saturn than was actually observed (*6*).

Figure 4 is a plot of peak current versus time of one of the outermost electrometer detectors of the medium-resolution analyzer for the period when convecting plasma ion currents were observed within Saturn's magnetosphere. The resulting profile has multiple maxima. The apparent decline of these fluxes inside 4.7 $R_S$ may be associated with the continuing decrease of the corotation speed with radial distance from Saturn. Throughout the radial distance range of Fig. 4, the corotation speed is below 80 km $sec^{-1}$, whereas the lower limit of the experiments' energy range corresponds to 140 km $sec^{-1}$ for protons. Since this experiment measures energy per unit charge, $E/Q$, response to corotation seems more compatible with ions of higher mass. Nevertheless, the locations of individual maxima appear to correspond roughly to the radial distances of several of Saturn's inner satellites. The highest peak is near the distance of Tethys, with perhaps a third maximum at the distance of Enceladus. One may speculate that the plasma has a source associated with these bodies, such as sputtered or photodissociated ices.

The high-resolution analyzer is equipped with two CEM detectors intended for more sensitive measurements of hot, diffuse planetary magnetospheric plasmas than are possible with the primary array of sensors employed for three-dimensional observations of solar wind ions. The corresponding fields of view for these two CEM detectors are located at the two edges of the field of view of the quadrispherical electrostatic analyzer. The angle between the directions of these fields of view and the spacecraft spin axis is 50.4°. Larger entrance apertures and longer accumulation periods are employed to improve the sensitivities of these two sensors. The accumulation period is approximately half the spin period of the spacecraft. Hence the field of view, including sweeping during accumulation, is a thin surface of a half-cone with half-angle 50.4°. Responses of these sensors for the two half-cones are telemetered for each of 64 energy passbands that span the $E/Q$ range from 100 V to 8 kV. Detectable plasmas were encountered on the inbound passage of Pioneer 11 from just inside the magnetopause at approximately 17 $R_S$ to just inside the orbit of Enceladus at approximately 4 $R_S$.

The electrostatic analyzer directly provides a measurement of $E/Q$ for the ions but does not identify the species. However, for a corotating plasma it is also possible to determine the mass per unit charge, $M/Q$, of the ions if the bulk of the ion velocity distribution can be approximated with a convecting, isotropic Maxwellian. Without such a determination of $M/Q$, accurate assessment of the temperature, $T$, and number density, $N$, is not possible. We are in the process of fitting the observed responses of the plasma analyzer to the parameters $T$, $N$, and $M/Q$ for all measurements within the dayside Saturn magnetosphere. The instrument is assumed to be responding

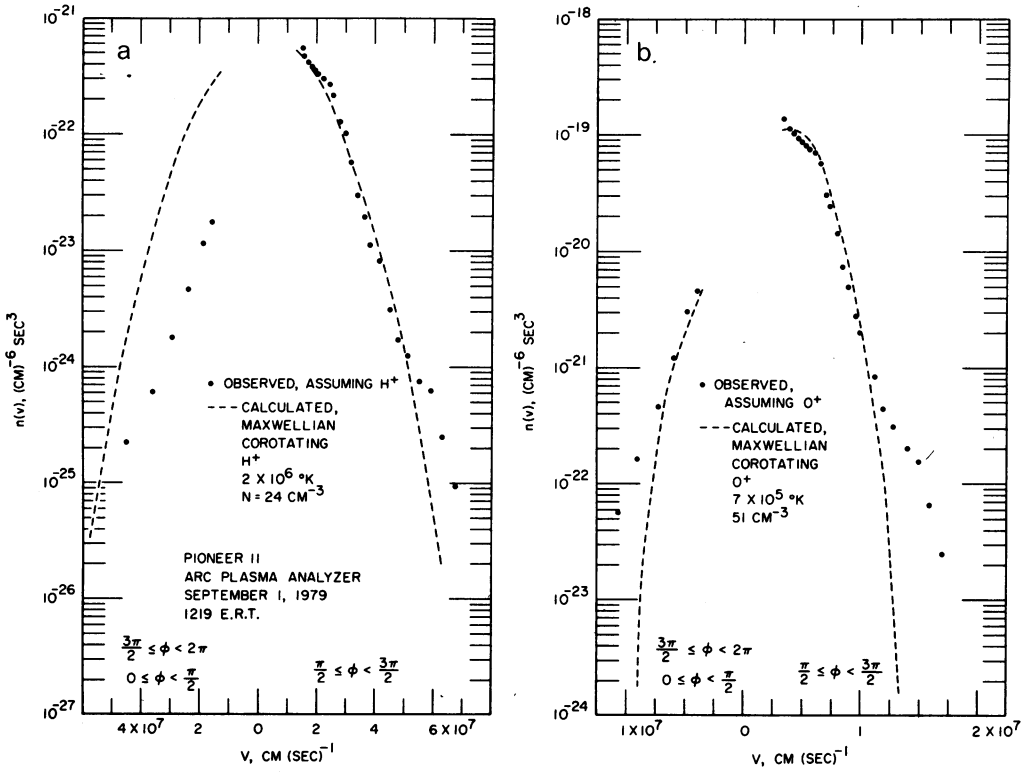


Fig. 5. Velocity distributions $n(v)$ computed for 1219 ERT on 1 September 1979 at a Saturn-centered radial distance of 6.3 $R_S$. These velocity distributions are dependent on the assumed ion species. (a) Velocity distributions (•) corresponding to an ion population of protons ($M/Q$ = 1); (b) velocity distributions corresponding to analyzer responses to $O^+$ ($M/Q$ = 16). Dashed lines summarize the expected responses of the analyzer to corotating Maxwellian velocity distributions.

primarily to a single-component, corotating, isotropic Maxwellian, and the best fit of the data to the three parameters above is found by numerically integrating the sensor responses over the two half-cones as functions of ion velocity and for various species, $M/Q$.

An example of these measurements and analyses is shown in Fig. 5 for 1219 UT, ERT, on 1 September 1979. The corresponding Saturn-centered radial distance of the spacecraft is 6.3 $R_S$. Figure 5a shows the positive-ion phase space densities as a function of ion velocity if the dominant responses of the analyzer are due to protons. These measurements are indicated as solid dots and the measurements for the two half-cones are indicated by $\pi/2 \leq \phi < 3\pi/2$ and $3\pi/2 \leq \phi < 2\pi$, $0 \leq \phi < \pi/2$, respectively, where $\phi$ denotes the clock roll angle of the spacecraft. In general, the velocity distribution function $n(v)$ is a monotonically decreasing function of velocity within the range sampled by the analyzer. Background counting rates were subtracted from the analyzer responses in computing the velocity distribution. Peak analyzer responses are approximately a factor of 80 above background rates. For the half-cone $3\pi/2 \leq \phi < 2\pi$, $0 \leq \phi < \pi/2$ the average responses for three energy passbands are used to improve counting statistics.

Also shown in Fig. 5a are the results of the fit of these data to a corotating Maxwellian distribution of protons. The corresponding temperature and density are $2 \times 10^6$ K and 24 cm$^{-3}$. The method for finding the best fit requires that the half-cone with best counting statistics, $\pi/2 \leq \phi < 3\pi/2$, be used to determine $T$ and $N$ at low velocities, $\lesssim 4 \times 10^7$ cm sec$^{-1}$. It is easily seen that the assumption of protons ($M/Q = 1$) provides a poor fit to the entire set of measurements. This procedure is repeated for each species $M/Q = 2$, 4, 8, 16, and 32. The best fit for this series of observations is $M/Q = 16$ with $T$ and $N$ equal to $7 \times 10^5$ K and 51 cm$^{-3}$, as shown in Fig. 5b. In fact, considering that this is only a three-parameter fit to the observations, the agreement is excellent, excluding only the high-velocity tail of the distribution, which may be due to either a nonthermal component of the distribution or another species. The current accuracy for assessing the $M/Q$ value of these ions is ± 4—that is, 16 ± 4—in our preliminary analysis. Although we have labeled these ions $O^+$, any positive ion, such as $OH^+$, within this $M/Q$ range can be equally well identified as the dominant ion. The elimination of $H^+$ as the ion species would seem to preclude the solar wind or the Saturn ionosphere as the main source of magnetospheric plasmas at 6 $R_S$. The $O^+$ or $OH^+$ could be produced by dissociation of ice on the rings or satellites. Heavier ions such as $S^+$ and $Na^+$, found in the magnetosphere of Jupiter and presumably associated with the Io volcanoes (*7*), do not appear to be a dominant constituent of the Saturn plasmas examined to date. This preliminary analysis will be followed by a comprehensive report covering the entire series of measurements of Saturn magnetospheric plasmas.

*Conclusions*. It is concluded that, like Earth and Jupiter, Saturn has a detached, strong, bow shock wave and a magnetopause. From the preliminary results it appears that Saturn's magnetosphere, like that of Jupiter, is very responsive to changes in the solar wind dynamic pressure, but on a scale size perhaps one-third of that at Jupiter. Also, Saturn's outer magnetosphere, like Jupiter's, is inflated by corotating plasma. The corotating plasma was not observed by this experiment during either of the Pioneer Jupiter encounters, presumably because of the much less favorable viewing directions and much higher backgrounds resulting from the more intense energetic charged particle environment at Jupiter.

It is interesting to note that the character of Saturn's magnetosphere should be drastically altered (expanded because of the reduction in solar wind dynamic pressure) when Saturn is near solar alignment with Jupiter such that Jupiter's long magnetospheric tail, observed by the Pioneer 10 plasma analyzer at the orbit of Saturn in March 1976 (*8*, *9*), engulfs Saturn. This may be just the situation for the Voyager 2 encounter with Saturn in August 1981 (*10*).

J. H. WOLFE, J. D. MIHALOV
H. R. COLLARD, D. D. MCKIBBIN
*Space Science Division,*
*NASA/Ames Research Center,*
*Moffett Field, California 94035*
L. A. FRANK
*Department of Physics and Astronomy,*
*University of Iowa,*
*Iowa City 52240*
D. S. INTRILIGATOR
*Physics Department,*
*University of Southern California*
*Los Angeles 90007*

**References and Notes**

1. J. H. Wolfe, J. D. Mihalov, H. R. Collard, D. D. McKibbin, L. A. Frank, D. S. Intriligator, *J. Geophys. Res.* **79**, 3489 (1974).
2. J. D. Mihalov, H. R. Collard, D. D. McKibbin, J. H. Wolfe, D. S. Intriligator, *Science* **188**, 448 (1975).
3. J. W. Dyer, *ibid.* **207**, 400 (1980).
4. S. M. Krimigis *et al.*, *ibid.* **206**, 977 (1979).
5. M. Dryer, A. W. Rizzi, W. Shen, *Astrophys. Space Sci.* **22**, 329 (1973).
6. E. J. Smith, L. Davis, Jr., D. E. Jones, P. J. Coleman, Jr., D. S. Colburn, P. Dyal, C. P. Sonett, *Science* **207**, 407 (1980).
7. S. M. Krimigis *et al.*, *ibid.* **204**, 998 (1979).
8. NASA/Ames Research Center, press release 76-22, March 1976.
9. D. S. Intriligator, H. R. Collard, J. D. Mihalov, O. L. Vaisberg, J. H. Wolfe, *Geophys. Res. Lett.* **6**, 585 (1979).
10. F. L. Scarf, *J. Geophys. Res.* **84**, 4422 (1979).
11. We thank the Pioneer Project Office at Ames Research Center, and in particular R. P. Hogan, for their effort and support during the Pioneer 11 Saturn encounter. We also thank the TRW Systems group for the spacecraft design and construction and Ball Aerospace Systems Division, Western Laboratories, for the design and construction of the Ames Research Center plasma analyzer experiment.

3 December 1979

## Saturn's Magnetic Field and Magnetosphere

Abstract. *The Pioneer Saturn vector helium magnetometer has detected a bow shock and magnetopause at Saturn and has provided an accurate characterization of the planetary field. The equatorial surface field is 0.20 gauss, a factor of 3 to 5 times smaller than anticipated on the basis of attempted scalings from Earth and Jupiter. The tilt angle between the magnetic dipole axis and Saturn's rotation axis is < 1°, a surprisingly small value. Spherical harmonic analysis of the measurements shows that the ratio of quadrupole to dipole moments is < 10 percent, indicating that the field is more uniform than those of the Earth or Jupiter and consistent with Saturn having a relatively small core. The field in the outer magnetosphere shows systematic departures from the dipole field, principally a compression of the field near noon and an equatorial orientation associated with a current sheet near dawn. A hydromagnetic wake resulting from the interaction of Titan with the rotating magnetosphere appears to have been observed.*

The similarity of Saturn to Jupiter and the somewhat tentative observations of decametric radio bursts from Saturn led to the expectation that the planet would have a relatively strong magnetic field. However, Pioneer 11 reached a distance of only 23.7 $R_S$ before the first bow shock crossing was observed. This is shown in Fig. 1, which presents an overview of the encounter as evident in the magnitude of the ambient magnetic field. Knowledge of the solar wind pressure (*1*), which was


0036-8075/80/0125-0407$00.75/0 